AIAA AVIATION Forum
August 2-6, 2021, VIRTUAL EVENT
AIAA AVIATION 2021 FORUM

10.2514/6.2021-3002

Aspects of analysis and simulation of a wing ditching scenario

Argiris Kamoulakos[1]
MH370-CAPTIO Team Member, Paris, France (akamoulakos@yahoo.com)

This paper is a follow-up of the paper titled "Aspects of analysis and simulation of a flaperon ditching scenario" presented in the Aviation Forum 2020, which proposed a modified definition of the added-mass in the Von-Karman-wedge water impact theory. It is again inspired by the recovery of the MH370 Boeing 777 right wing flaperon debris and the associated speculation of a possible failed ditching. The limitations of the previous publication regarding only bodies with infinite mass is removed and the proposed modified added mass version of the Von Karman theory is reworked for a flat plate of finite mass. This leads to a new set of simple analytical relations for the evolution of the hydrodynamic force with depth of immersion as a function of the plate horizontal and vertical speeds and the angle of impact. The analytical estimates of the hydrodynamic force at first impact and beyond were validated numerically through simulations with the Smoothed Particle Hydrodynamics (SPH) method and were found very encouraging. The existence of an equivalence between the hydrodynamic force evolution for ditching and an "equivalent" vertical slamming is re-established through analytical means and demonstrated through simulation. Finally, the analytical expressions for the hydrodynamic force versus depth of immersion thus obtained were applied to a simplified elastic B777-type wing model in ditching in order to estimate the maximum tip deflections thus providing a conservative envelope of horizontal and vertical speed ditching combinations that can compromise its structural integrity.

I. Nomenclature

α	=	angle of inclination of the under-surfaces with the horizontal (angle of deadrise)
C_α	=	pressure coefficient due to trailing edge end-effects
F_v	=	vertical component of the resultant pressure force acting on the body
l	=	length of the body
m	=	mass per unit length of the body
M	=	total mass of the body
M_p	=	total mass of the plate
V_0	=	initial vertical (impact) speed of the body
V	=	instantaneous vertical speed of the body
V_{x0}	=	initial horizontal ditching speed
V_{y0}	=	initial vertical ditching speed
V_n	=	equivalent ditching speed normal to the instantaneous water surface
x	=	half width of the wedge at the plane of the undisturbed water surface
x_{eff}	=	effective half width of the wedge for added mass estimation
y	=	depth of immersion normal to the plane of the undisturbed water surface
δ_{tip}	=	wing tip deflection in vertical direction
I	=	impulse from impact
ω_f	=	flapping frequency of the wing
μ	=	participating mass of the wing under flapping mode

[1] Scientific Director, ESI Group, 3 bis rue Saarinen, 94528 Rungis, FRANCE.

II. Introduction

"On 07 March 2014 at 1642 UTC a Malaysia Airlines (MAS) Flight MH370, a Beijing-bound international scheduled passenger flight, departed from Runway 32R, KL International Airport [KLIA] with a total of 239 persons on board (227 passengers and 12 crew). The aircraft was a Boeing 777-200ER, registered as 9M-MRO." (extract from the Malaysian accident investigation report).

A little bit later that day the aircraft vanished from the radars. Ever since, its whereabouts remain a mystery.

In the years that followed, a very limited amount of debris has been recovered in the Indian ocean coastal lines of Africa, Mauritius and Isle de Reunion. From this debris, only three pieces have been formally identified as definitely belonging to that aircraft: the right flaperon, the right inner flap and the trailing edge of the left outer flap.

Despite extensive search, no traces of the aircraft itself have been found and the case is (at least for now) closed after the final accident investigation reports from Malaysian authorities in 2018.

Many scenarios have been proposed regarding what happened to this aircraft.

The CAPTIO team has put forward a coherent account of the possible trajectory the aircraft would had followed, that satisfies as much as possible the available satellite and Air Traffic Control data, and it leads to a potential ditching close to the Christmas Islands. The details of this work can be found in the CAPTIO website http://mh370-captio.net/.

The recovered confirmed debris of this flight holds the key to the aircraft final moments. In particular, the flaperon debris which has been extensively examined by the Direction Générale de l' Armement (DGA) Ministry of Defense in France [1] and is pictured in Fig. 1, during its transfer for investigation.

Fig. 1 Flaperon being recovered by the French authorities at Ile de La Réunion.

What is very intriguing is the missing part of the trailing edge. The conclusion of the French report was that a ditching process was the most probable cause. The author who is a member of the CAPTIO team embarked to complement the DGA study by attempting to examine (as much as possible with the available data) the validity of the ditching assumption from a theoretical and a numerical (simulation) point of view. The findings were published in [2].

As the separation of the flaperon from the wing under such a scenario is suspected to be due to wing rupture, the ditching process of a wing is examined in this paper in a similar way as in [2].

III. Strategy for modelling ditching through numerical simulation

Ditching involves fluid-structure interaction with large topology changes of the fluid because of the creation of waves during the penetration by the structure. One practical way to simulate ditching is to model the fluid with a particles method in order to allow large topological changes and mixing, that is, phenomena that are very difficult to be captured by traditional numerical methods, like the Finite Element method (FE) for instance. The particles method that was used to model the fluid (water) was the Smoothed Particle Hydrodynamics method (SPH). See Fig. 2 below for basic concepts.

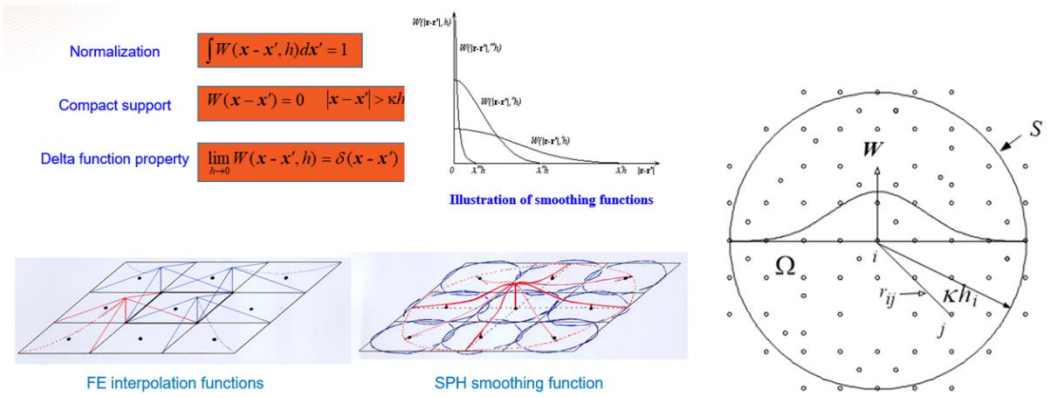

Fig. 2 Foundation of SPH idealizations as compared to FE

In order to choose the appropriate discretization of the fluid domain for ditching, a systematic investigation of the Von Karman wedge benchmark was done. The problem setup is as in Fig. 3 below corresponding to an infinitely long horizontal prismatic body with a wedge-shaped undersurface impacting vertically a semi-infinite fluid domain.

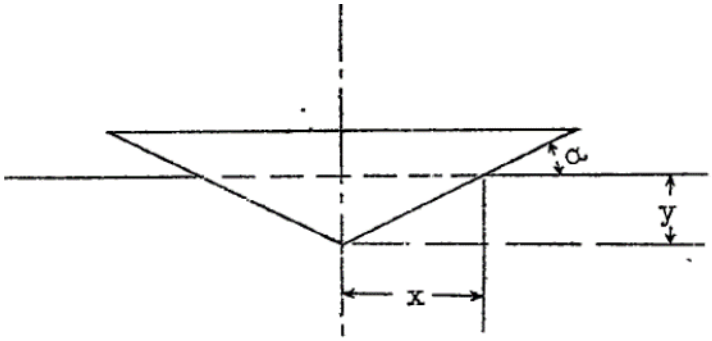

Fig. 3 Definition of the Von Karman wedge from [3]

The problem is essentially 2D as the third dimension that goes to infinity is self-similar, hence the problem corresponds to the class of "plane strain" problems.

The simulations were done using the explicit transient dynamic code PAMCRASH of ESI Group [10] and using the 2D and 3D options for SPH modelling, as required. The material model for the water requires an appropriate Equation Of State (EOS). Although traditionally a polynomial EOS is used for water under impact, since in ditching (under the velocities we are interested) the water compressibility is very small, it is more efficient to adopt the Murnahan-Tait EOS [3,10].

Before proceeding with the simulations, the necessary theoretical foundation is presented below, and the PAMCRASH-based simulations are used to validate and complement this foundation.

IV. Basic Von Karman theory for water impact of seaplane floats

Von Karman [4] examined the problem of an infinitely long horizontal perfectly rigid prismatic body with a wedge-shaped undersurface as it strikes vertically an infinitely long horizontal undisturbed surface of water in order to calculate analytically an estimate of the force per unit length acting between the body and the water at "first impact" stages. In his pioneering approach, he ignored the subsequent hydrodynamic flow effects, the viscosity or cavitation effects, any horizontal relative velocity to the sea and finally the "Archimedes" force (buoyancy), as he was interested at the "first impact" scenario.

In this sense the problem is tackled from a "conservation of momentum" approach between the before impact and after impact state of the system, without any gravitational effects and in 2D.

Let m be the mass per unit length of the body (seaplane), α the angle of inclination of each of the wedge undersurfaces with the horizontal and y the vertical distance the body travels in time from the initial point of impact with the water (depth of immersion). The time varying motion of the body within the water will provoke a disturbance in a mass of water beneath it, which will provide inertial resistance to the penetration. This is the "virtual mass". Von Karman, using the 2D assumption, estimated the virtual mass to be equal to the mass of water contained in a semi-cylinder of diameter equal to the width of the wedge at the plane of the undisturbed (original) water surface.

The semi-cylindrical assumption for the virtual mass comes from the fact that a flat plate in 2D, fully immersed in a fluid and accelerating through it, experiences theoretically an added inertia from a mass of fluid that is contained within a circular cylinder of diameter equal to the width of the plate. The rear part of the plate experiences a suction force from the rear semi-cylinder of water while the front part a compression force from the forward semi-cylinder of water. In our case we have half the domain filled with air and half with water, hence only the semi-cylinder of water represents any added inertial force.

The conservation of momentum at any time t during the penetration then gives:

$$mV_0 = mV + \frac{1}{2}\pi x^2 \rho V \tag{1}$$

where ρ is the water density and V_0 the initial vertical speed. Setting the following for the instantaneous velocity:

$$V = \frac{dy}{dt} = \tan\alpha \cdot \frac{dx}{dt} \tag{2}$$

and using the following identity:

$$\frac{d^2x}{dt^2} = \frac{d}{dx}\left[\frac{1}{2}\left(\frac{dx}{dt}\right)^2\right] \tag{3}$$

we can substitute Eq. (2) in Eq. (1) and using Eq. (3) we can obtain for a body with an out-of-plane length l and total mass M, the instantaneous retardation as below:

$$\frac{d^2y}{dt^2} = \frac{{V_0}^2 \cot\alpha}{M\left(1+\frac{\rho l\pi x^2}{2M}\right)^3}\rho l\pi x \tag{4}$$

The associated vertical force F_v can then be obtained from Newton's law as:

$$F_v = M\frac{d^2y}{dt^2} = \frac{{V_0}^2 \cot\alpha}{\left(1+\frac{\rho l\pi x^2}{2M}\right)^3}\rho l\pi x \tag{5}$$

A. The Wagner correction and its modification by the author

Wagner [5] examined the same problem by trying to take account of the wave generated by the body during its immersion in the water. Since the water displaced by the immersing body rises along its sides, the width of the wetted surface and the associated mass of the flow should be greater than those based on the flat width in the plane of the undisturbed surface, as Von Karman assumed.

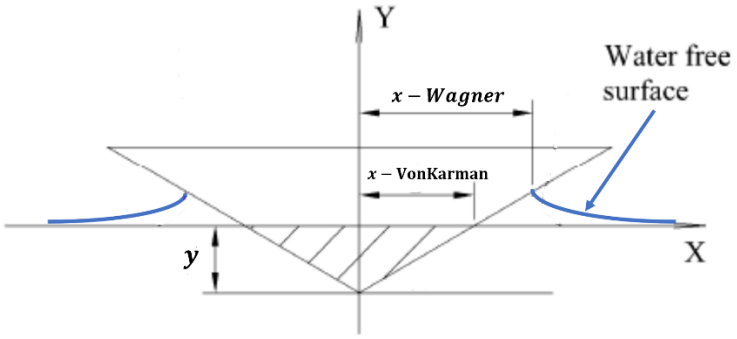

Fig. 4 Definition of the Wagner "correction"

Assuming that the water particles at the top of the water upflow move vertically up (see Fig. 4) and in accordance to the analytical 2D velocity profile for the water crest at the interface with an inclined flat plate being immersed in a horizontal water surface, he determined the "effective" width of the wedge at the tip of the wetted surface. He discovered that for a triangular cross section, which is the case for the wedged shape undersurface of Von Karman, that it is 1.57 (or $\frac{\pi}{2}$) times larger of that by Von Karman.

This is sometimes termed as the "Wagner correction", although it is not sure that Wagner was aware of Von Karman's work as his approach was independent and different.

Wagner proceeded to re-estimate the "virtual mass" of the fluid based on this risen wetted surface and this was consequently estimated as $\left(\frac{\pi}{2}\right)^2$ of that by Von Karman. This implied also that the resultant vertical force would be scaled by $\left(\frac{\pi}{2}\right)^2$ as compared to that of Von Karman.

However, over the years it became evident that while Von Karman's formula in equations Eq. 4, Eq. 5 and Eq. 6 underestimated the resultant vertical force during immersion, the Wagner correction produced a force that greatly overestimated this force as compared to experimental measurements.

Researchers like Mayo [6] gave a great account of the differences between the Von Karman and Wagner theory and all the efforts done to reconcile them, and all actually came down to a large effect to the definition of the added mass.

The author believes that Von Karman's estimation for the added mass appears to have a good theoretical foundation as a first guess, since at that time the means at his disposal were very limited. However, Wagner's extension of basing the added mass on a cylinder whose radius is the "effective" width of the wedge at the tip of the wetted surface, appears not justifiable, as the fluid near the tip of the wetted surface is already part of the "spray" and is already moving tangentially, thus has already delivered its momentum to the wedge. Hence a cylinder thus defined will include much more fluid mass than the one that should be moving downwards with the plate.

Payne [9] is one to seriously challenge the choice of added mass size by Wagner, in favour of that of Von Karman and in the process he quotes amongst other researchers the experimental results of Bisplinghoff at MIT in the 60s. These results showed that the actual "effective" width of the wedge (excluding spray which is physically present) should be on average between 1.2 and 1.35 times larger than that of Von Karman.

In this paper we have no experimental results but we use high fidelity simulations (PAMCRASH code) for our work which include the spray and we have found that the best factor for correcting the Von Karman effective wedge width was about 1.25, and the corresponding hydrodynamic force comparisons for all cases of interest in this article were very encouraging, as it will be shown in the rest of the paper. Since 1.25 is practically $\sqrt{\frac{\pi}{2}}$ and for the sake of similarity with the existing equations we can define the effective wedge width for added mass definition as:

$$x_{eff} = \sqrt{\frac{\pi}{2}}\, x_{VonKarman} \tag{6}$$

The consequence of the above is that the added mass now will be scaled by $\frac{\pi}{2}$ as compared to that of Von Karman and similarly the corresponding hydrodynamic force. Substituting Eq. (6) to Eq. (1) for x and repeating the derivation of the hydrodynamic force we get:

$$F_v = \frac{\pi^2}{2} V_0^{\,2} \frac{\rho l x \cot\alpha}{\left(1+\frac{\rho l \pi^2 x^2}{4M}\right)^3} \tag{7}$$

It is very challenging to visualize the added mass in ditching but one "imaginative" way through simulation can be to depict the part of the fluid that moves downwards with the body at any given instant.

A wedged object was modelled as a rigid body using the PAMCRASH code and it impacted a stationary mass of water (modelled with SPH 2D technology as explained earlier).

The geometry of the wedge was such it makes an angle of 30 degrees with the undisturbed surface of the water and the prescribed immersion speed was 10 m/s.

Figure 5 below attempts to show the added masses based on the Von Karman (yellow), Wagner (blue) and the author (red).

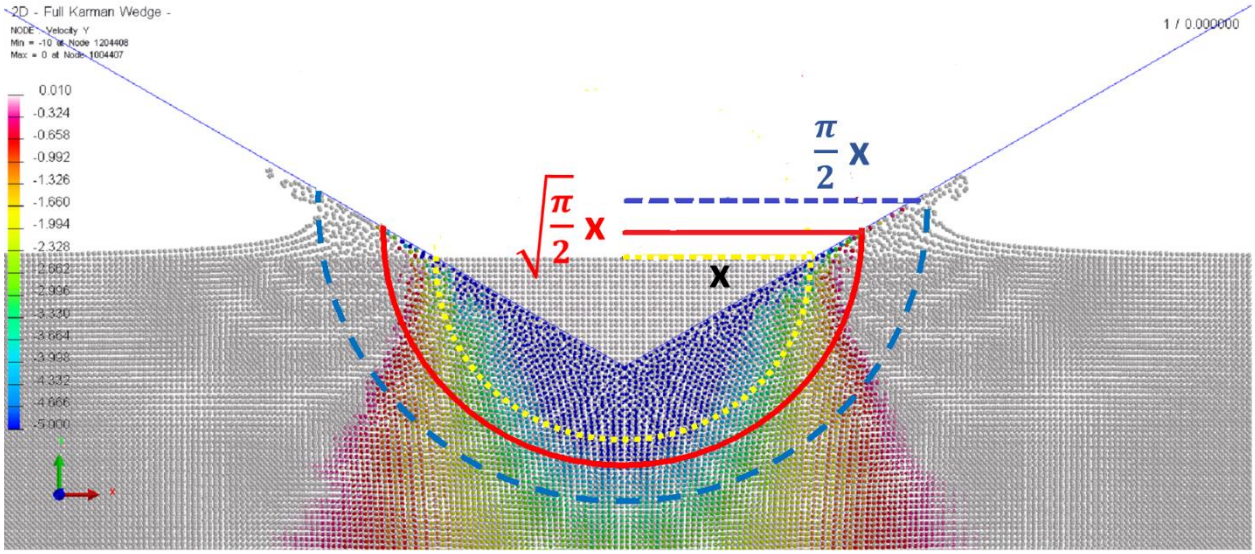

Fig. 5 Added masses according to Von Karman (yellow), Wagner (blue) and the author (red)

The initial undisturbed fluid is shown in order to allow the definition of the Von Karman added mass that uses the undisturbed surface as reference.

It can be seen that the Von Karman added mass (based on x) does not include some of the fluid that moves significantly downwards and certainly not any part from the water elevation at the crest, by definition, while the Wagner added mass (based on $\frac{\pi}{2}x$) contains a lot of fluid that is not moving downwards or is moving within the "spray" at the crest that is not part of the added mass, as shown by Bisplinghoff.

The definition from the author (in red, based on $\sqrt{\frac{\pi}{2}}x$) extends the Von Karman added mass to include parts of the fluid still participating in the downward motion plus includes the effective width of Bisplinghoff (the part of the crest that has contour colours showing vertical motion), hence it is a reasonable compromise and hints visually to why the results of this paper shown later on are encouraging.

The wedge numerical (SPH) model presented above was subjected to a vertical impact of 2.65 m/s with a variable mass of 1.5 kg, 4 kg and 8.6 kg. The evolution of the vertical force as a function of the immersion y of the wedge is displayed in Fig. 6, 7 and 8 as compared to the theoretically predicted force from Eq. (7).

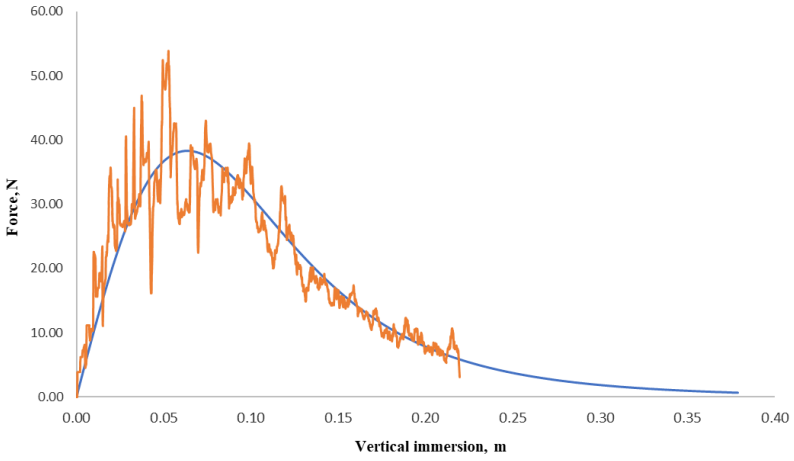

Fig. 6 Force versus immersion depth comparison between simulation and theory – 1.5 kg wedge

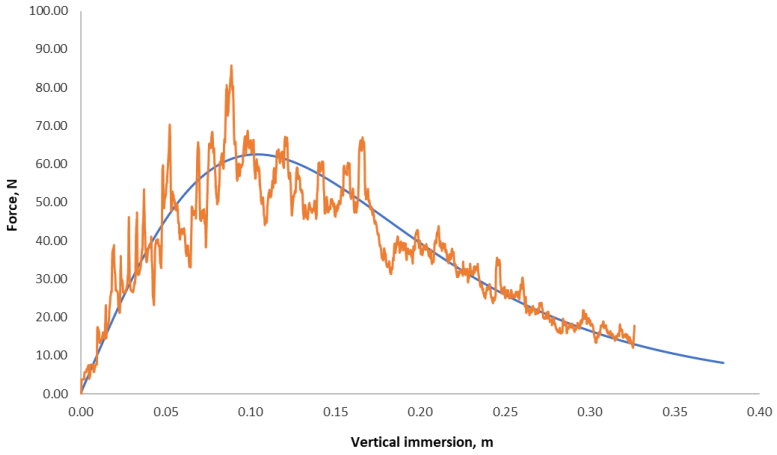

Fig. 7 Force versus immersion depth comparison between simulation and theory – 4 kg wedge

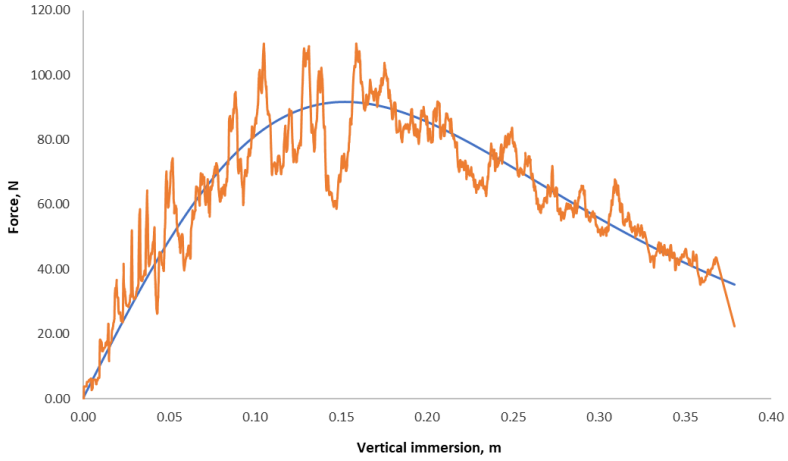

Fig. 8 Force versus immersion depth comparison between simulation and theory – 8.6 kg wedge

V. Adaptation of the Von Karman theory to a flat plate at vertical impact

Noting that an inclined flat plate under vertical impact resembles half the Von Karman wedge, one can assume that the associated vertical force evolution during vertical immersion will basically be half the force predicted by the Von Karman wedge but adjusted by a coefficient that represents the force reduction due to the end-effects. This is to compensate for the change of flow around the lowest end of the plate which is no longer the apex of a wedge but an open end.

Important point is that M in Eq. (7) is the total mass of the equivalent Karman wedge and this is double the mass of the flat plate M_p.

$$M = 2M_p \tag{8}$$

Hence dividing Eq. (7) by 2 and using Eq. (8) we get:

$$\boldsymbol{F_v = C_\alpha \left(\frac{\pi}{2}\right)^2 V_0^{\,2} \frac{\rho l x \cot\alpha}{\left(1+\frac{\rho l \pi^2 x^2}{8M_p}\right)^3}} \tag{9}$$

where $C_\alpha$is a coefficient that is inclination dependent and modifies the force according to its end-effects and to any minor adjustments regarding to the choice of Eq. (7) for the effective wedge width.

The coefficients C_α were previously obtained by the author [2] as a function of inclination α :

$$C_\alpha \sim 1.3561 - 0.206 \ln \alpha_{in\ degrees} \tag{10}$$

or

Table 1 Evolution of C_α versus α

α (degrees)	C_α
15	$\frac{16}{20}$
30	$\frac{13}{20}$
45	$\frac{11.5}{20}$

The reason for introducing the coefficient C_α is shown pictorially in Fig. 9 which exposes the different flow around the apex of the plate as compared to the original wedge. (see Kamoulakos [2])

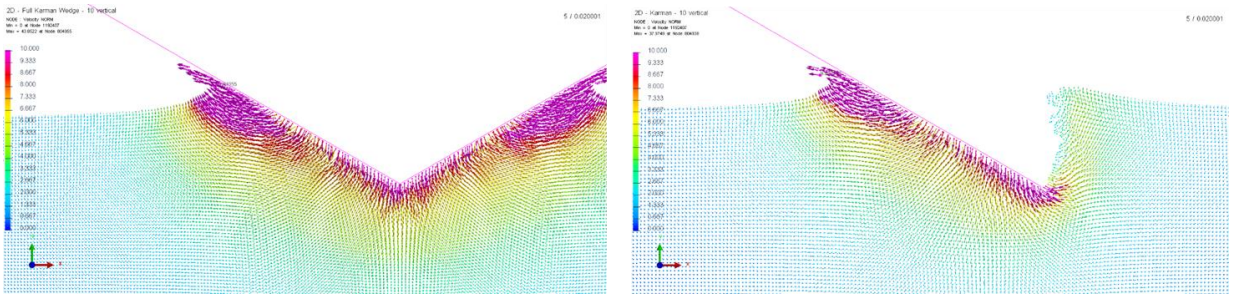

Fig. 9 Velocity vector contours for the Von Karman wedge and flat plate vertical impact

The flat plate in the above configuration (30 degrees inclination) was simulated under initial vertical speed of 41.76 m/s and 4 kg mass. The evolution of the vertical force as a function of the immersion y of the plate is displayed in Fig. 10 as compared to the theoretically predicted force from Eq. (9).

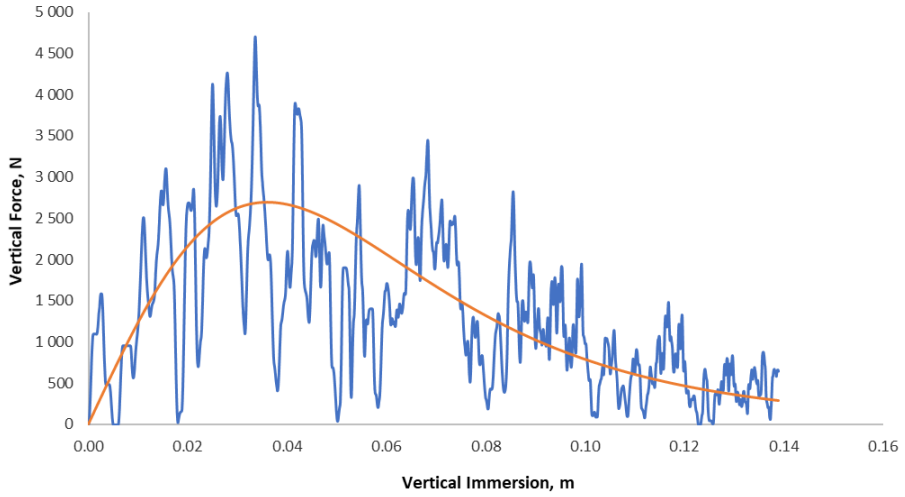

Fig. 10 Force versus immersion depth comparison between simulation and theory – 4 kg plate

VI. Adaptation of the Von Karman theory to a flat plate at inclined impact

For a vertical immersion of a wedge, it is obvious that the only velocity that matters is the vertical one and the pressure applied to the wedge surfaces during immersion has a zero resultant in the horizontal direction due to symmetry, while only the vertical force component on the two surfaces matters and it is additive.

However, this is not the case for a half wedge, ie, a flat plate, the resultant pressure from the flow field evolution will have a horizontal and vertical resultant force. Equation (9) will provide only the vertical force based on Von Karman's theory, since it was obtained from vertical momentum conservation only.

Considering what kinematics disturb the water and provide the flow around the plate one can see that it is not the vertical velocity that really matters but the effective velocity normal to the plate which will disturb the flow and provoke the associated hydrodynamic forces. Under the assumptions of this paper, any inclined plate with a velocity vector aligned along the plate surface will enter the water like an arrow and "not disturb" the water (the thickness of the plate is not a geometric parameter, only its surface, and under these conditions it is invisible to the fluid).

We can rewrite Eq. (9) with respect to the vertical distance variable y as below:

$$F_v = C_\alpha \left(\frac{\pi}{2}\right)^2 V_0^{\,2} \frac{\rho l y (\cot\alpha)^2}{\left(1+\frac{\rho l \pi^2 x^2}{8M_p}\right)^3} \tag{11}$$

Defining the velocity component normal to the plate as:

$$V_n = V_0 \cos\alpha \tag{12}$$

and realizing that this velocity is the sum of the projections of the horizontal V_{x0} and vertical velocities V_{y0} of the plate as below:

$$V_n = V_{x0} \sin\alpha + V_{y0} \cos\alpha \tag{13}$$

we can rewrite Eq. (11) in the following form:

$$\boldsymbol{F_v = C_\alpha \left(\frac{\pi}{2}\right)^2 \left(V_{x0} + V_{yo} \cot\alpha\right)^2 \frac{\rho l y}{\left(1+\frac{\rho l \pi^2 x^2}{8M_p}\right)^3}} \tag{14}$$

Equation (14) gives us an estimate of the vertical force evolution on an inclined flat plate under inclined immersion due to **initial** (not prescribed) horizontal and vertical speeds of V_{x0} and V_{yo} respectively.

Furthermore, in the publication by Kamoulakos [2], an equivalence between inclined ditching and vertical immersion was demonstrated, for the "first impact" stage, that is, for the stage of monotonic vertical immersion (the part of the ditching where the object vertical velocity is downwards). The following table was quoted in [2] for flat plate inclination α of 30 degrees, containing an example of velocity combinations:

Table 2 Equivalence between inclined ditching and vertical immersion [2]

V_{x0} (m/s)	V_{y0} (m/s)	V_n (m/s)	V_0 (m/s)
55	**10**	36.16	**41.76**
55	20	44.82	51.75
50	30	50.98	58.87
68.42	2.54	36.41	42.04
68.42	5.08	38.61	44.58
70	20	52.32	60.41

To demonstrate the validity of Eq. (14), the above highlighted case of initial horizontal speed V_{x0} of 55 m/s and an initial vertical one V_{y0} of 10 m/s was examined and compared to the theory for only vertical immersion with initial vertical speed 41.76 m/s (zero horizontal speed at all times).

The simulation model of the flat plate inclined at 30 degrees was used to simulate the plate at the abovementioned inclined impact setup and the vertical force evolution from the simulation results is presented against the Eq. (14) one in Fig. 10 as below.

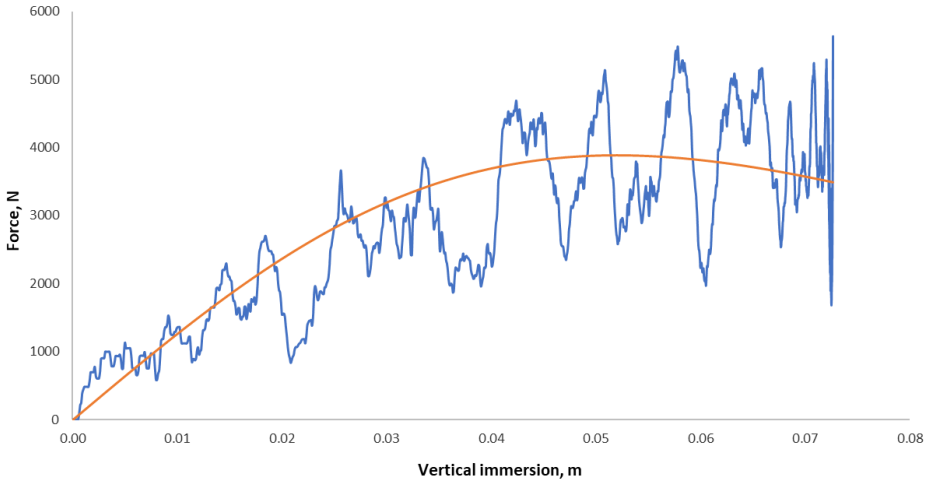

Fig. 11 Force versus immersion depth: blue 55 m/s horizontal – 10 m/s vertical speeds simulation, orange 41.76 m/s theory

We can see from Fig. 10 that the comparison is favorable.

To further examine the validity of the equivalence between vertical immersion (slamming) and inclined ditching, a model of a typical wing-type body was simulated. The model was obtained from public domain CAD data for a B777-type wing and it is reasonably representative for this type of exercise. The part from the engine outwards was modelled, with a span of 23.6 m which is roughly 2/3 of the B777 wingspan.

The wing was modelled as a "rigid body" to be compliant with this exercise, and it was placed horizontal with the inclination angle of 13 degrees. The sea was modelled by SPH particles.

Two simulations with PAMCRASH were done:

one with the ditching scenario of initial horizontal speed of 70 m/s and initial vertical speed of 3 m/s

one with the equivalent vertical slamming scenario of 19 m/s initial vertical speed (all other directions constrained) which is obtained from Eq. (12) and (13)

Figures (12) and (13) show the wing sea impact for those two scenarios as below:

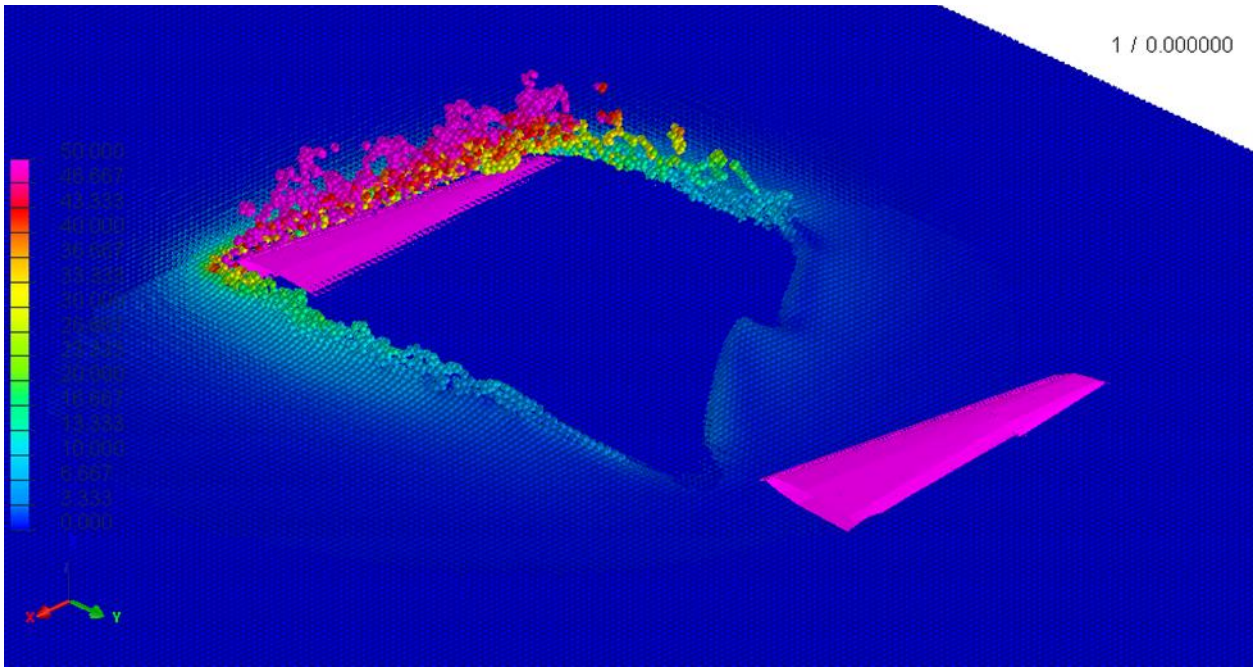

Fig. 12 Inclined ditching of a wing – initial and final position

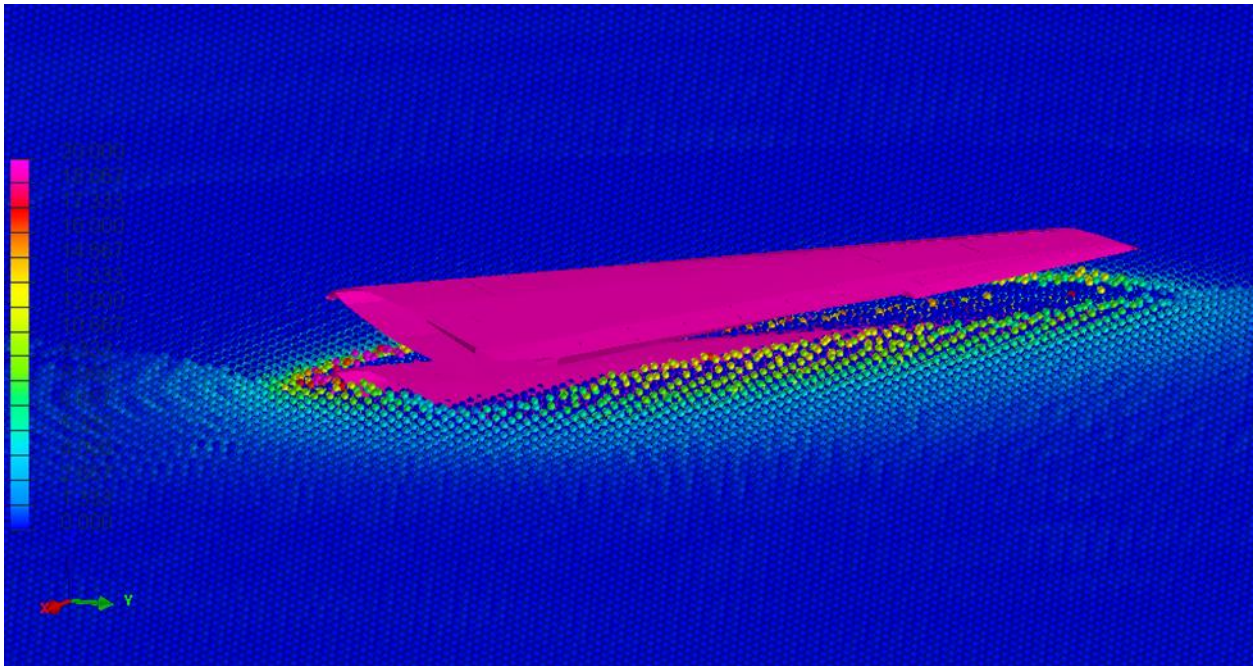

Fig. 13 Equivalent vertical slamming simulation of wing – initial and final position

Figure 14 shows the comparison of the corresponding vertical force evolution.

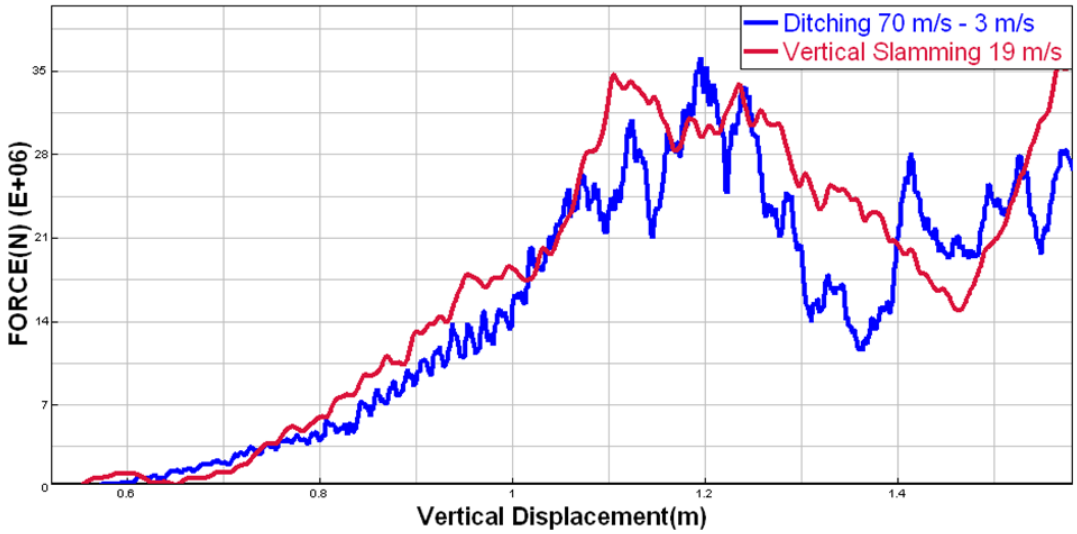

Fig. 14 Simulation results for vertical force versus depth of immersion evolution / Equivalence between inclined ditching and vertical slamming

It can been that the resultant vertical force evolution in the two cases is very similar, validating the fact that there is an equivalence between vertical slamming and inclined ditching, that is, for every combination of horizontal and vertical speeds in inclined water impact there is an equivalent vertical impact speed that produces very similar force evolution.

This observation allows us to reduce significantly the size of the simulation models when we want to obtain an order of magnitude of the "first impact" peak load and time duration in ditching, quantities that define the impulse upon the wing. The reduction in model size comes from the fact that we need to model only the sea adjacent to the wing and not the sea that participates in the planning of the wing in inclined ditching, which is quite disproportionately large and the corresponding modelling with SPH particles is very computer processing intensive (CPU).

Another observation is that the peak load can arrive very early on the structure during ditching. Figure 13 below shows the moment of peak load during the simulation of the above inclined ditching scenario.

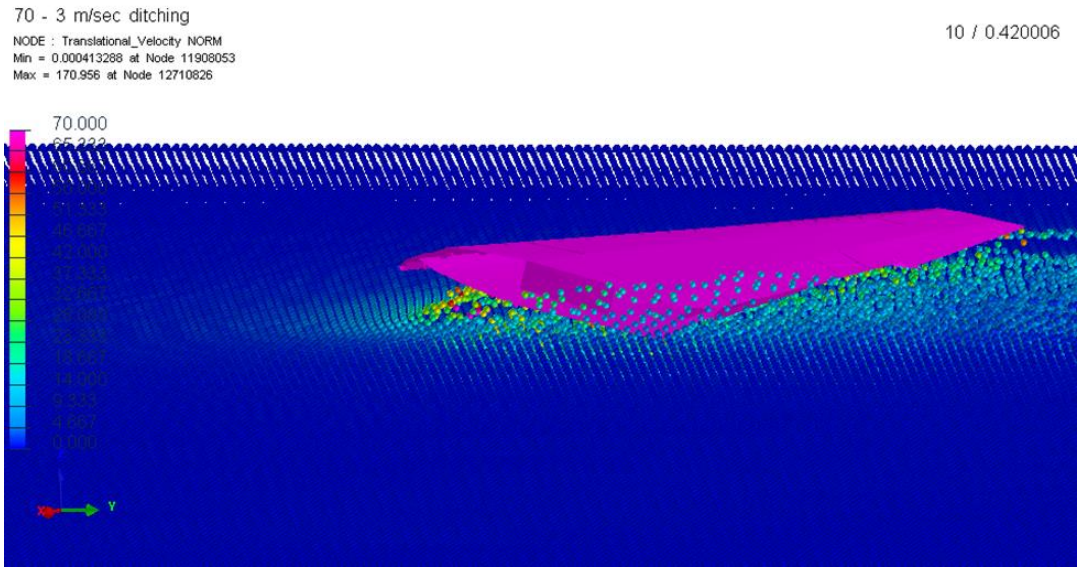

Fig. 15 Inclined ditching 70 m/s – 3 m/s, moment of maximum load

This observation allows us to have a reasonable order of magnitude of the impulse using a rigid model, as the wing elastic deformation that follows (which can be significant), will be to a good extend the consequence of this initial impulse.

The wing model was simulated with a very high mass, no gravity and a vertical speed of 15.34 m/s (which corresponds to the same inclined ditching speed setup but at 10 degrees inclination). The force versus vertical immersion force evolution is showed below in Fig. 16 and compared to the corresponding theoretical curve.

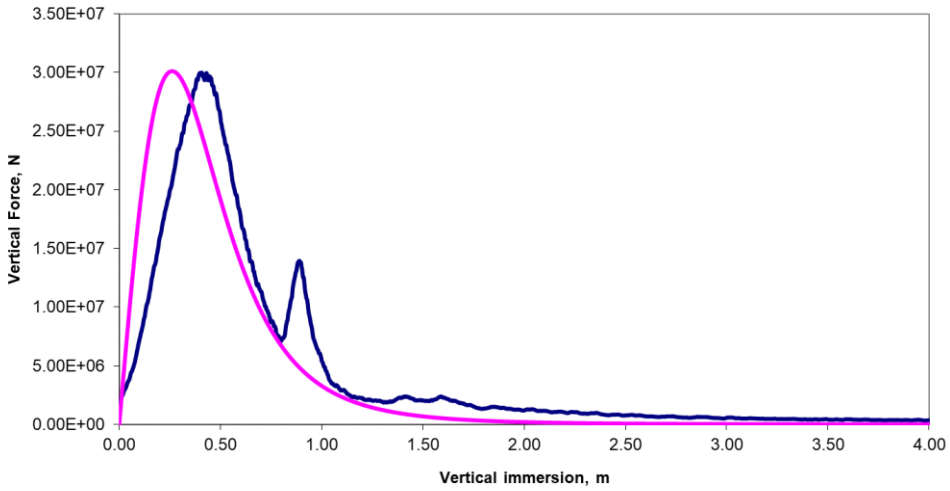

Fig. 16 Force versus immersion depth: blue 70 m/s horizontal – 3 m/s vertical speeds simulation, purple 15.34 m/s theory (vertical slamming)

It can be seen that the correspondence is quite good; the apparent shift in the curves is due to the fact that the theoretical result is obtained from the Von Karman theory where the entire plate is flat and at 10 degrees inclination, which is different from the wing used where the section has only an average inclination of 10 degrees and variable spanwise chord.

The above force-depth evolution, if plotted as force-time evolution, it will give the impulse upon the wing at "first impact" due to the ditching event. This will be presented in a follow-up publication.

VII. Linking to the Flaperon publication [2]

As mentioned in the introduction regarding the MH370 disappearance, the recovery of the right wing flaperon with the trailing edge missing implied the action of hydrodynamic forces. A "missed" (uncontrolled) ditching scenario appears as a credible one, possibly with a "right wing first impact" at a significant right-roll inclination.

In such a case the flaperon would impact the water with the prescribed motion of the wing, as the flaperon mass is negligible compared to that of the wing. This is the reason why in [2] the mass of the flaperon was considered infinite, so that it conveys the inertia of the wing during the ditching. The corresponding equations where adapted accordingly.

However, the impact of the wing with the water needs a combination of the wing mass and part of the aircraft mass in order to assess the forces upon ditching. This is because with a "right wing first impact" scenario, part of the aircraft inertia will pass through the wing (we do not assume a fuselage underbelly first impact). Hence the need to adapt the full Von Karman equations that include the mass of the impactor.

From all possible wing ditching scenarios, the admissible combinations of horizontal and vertical speeds are those that will result in the failure of the attached flaperon trailing edge in the way examined in [2]. Hence the need to combine the outcome of this paper with that of [2].

Further on, and for reasons beyond this publication, it appears possible that the recovered flaperon was separated from the wing due to wing rupture from excessive deformation / loads during this uncontrolled ditching.

In order to assess this, a simplified elastic model of the wing is needed, for "order of magnitude" analysis, as no numerical model of an elastic B777 wing is in our possession.

The wingbox obtained from Fig. 17 was parametrized using Engineer's Theory of Bending and Bedt-Batho theory in order to achieve a stiffness that can give about 1.9 m wing tip deflection at MTOW.

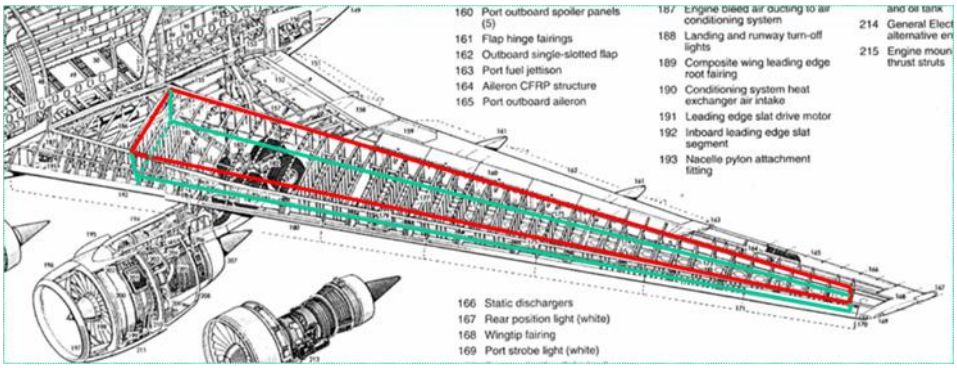

Fig. 17 Basis of B777 wingbox sectional properties for a simplified model that respects limit and ultimate loads response

The wing tip deflection at MTOW was estimated from the testing to failure of the B777 wing which is quoted as 24 ft at 1.54 limit load.

The estimated simplified spanwise variable flexural properties of the wingbox and associated mass distribution were used to make a 10 beam Finite Element model using the code ADBLST from Kamoulakos [14] which allows distinct center of area, center of mass and shear center at each section. The associated tip deflection from aerodynamic loads at MTOW was thus obtained.

Similarly, the wing eigen modes were obtained using the code ADBLDYN (Kamoulakos [14]) with a first wing flapping mode frequency ω_f (without the engine) of about 6.88 rad/s (1.1 Hz). This is the mode that would participate most during the ditching process under this level of approximation. The engine was not included as during a severe ditching event it will separate from the wing.

The wing was simulated as explained in the previous section under vertical impact for the range and combination of velocities that can produce rupture of the trailing edge of the flaperon (as defined by the equations of [2]). The triangular pulse upon impact (like in Fig. 15 but in time) would give the peak force and the duration, which gives the impulse I.

An order of magnitude of the tip deflection will then be obtained from Eq. (15).

$$\delta_{tip} = \frac{I}{\mu\omega_f} \tag{15}$$

where ω_f is the flapping frequency of the wing and μ the participating mass.

Wing fracture would then be expected as probable if δ_{tip} calculated from Eq. (15) is of the order of 24 ft or more (see Fig. 18).

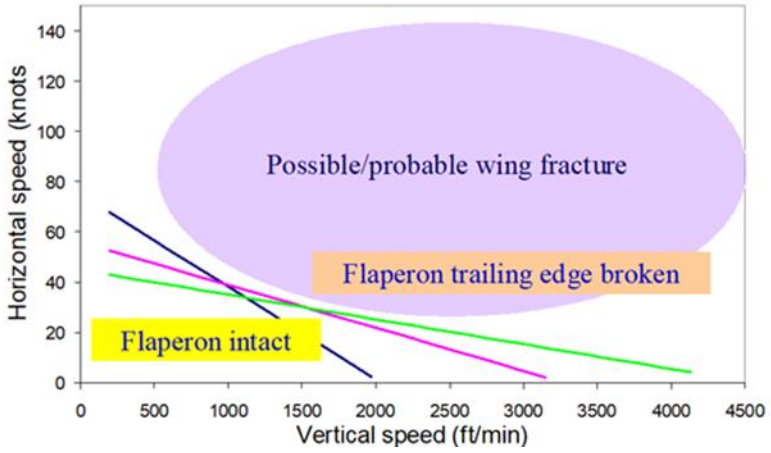

Fig. 18 Envelope of ditching scenarios for possible wing fracture

VIII. Conclusion

Motivated by the recovery of the MH370 Boeing 777 right wing flaperon debris and the associated suspicion that its damage was due to a ditching scenario, the author continued his previously published work on the flaperon [2] by assessing the forces exerted by fluid-structure interaction upon a wing-like body under ditching, both analytically and numerically.

In this respect the author modified the Von Karman water impact theory by suitably redefining the added mass estimation and adapting it to a wing-like body with a **finite** mass under ditching. He then obtained a simple analytical relation for the total hydrodynamic force as a function of horizontal and vertical speeds and angle of impact. Validation of the analytically obtained force to that obtained by Smoothed Particle Hydrodynamics (SPH) water simulations was very favorable.

The analytical work in this paper further confirmed the suggestion in [2] of the existence of an equivalence between inclined ditching and vertical slamming of a wing-like body with the relative speed normal to the water surface as the link. This is of significance as it allows to drastically reduce the sizes of the numerical models for parametric evaluation and the corresponding CPU usage, by modelling the sea in the vicinity of the wing (under equivalent slamming) and not all along its trajectory in ditching. It can have also value in devising simpler and smaller experimental setups for laboratory testing of ditching.

Finally, as far as the pursue of resolving the MH370 puzzle is concerned, the foundation was put in linking the envelope of wing responses under ditching to those that correspond to the flaperon damage in order to identify the most probable sea impact scenarios.

Acknowledgments

The author would like to acknowledge the support of the rest of the MH370-CAPTIO team, namely, Jean-Marc Garot, Jean-Luc Marchand, Michel Delarche and Philippe Gasser, who have pioneered a coherent hypothesis on the MH370 enigma. It has to be noted that the author's work, like the work of the rest of the team, is voluntary, benevolent and represents only the views of MH370-CAPTIO and nobody else's.

Finally, the author, whose personal research in this paper does not involve in any way ESI Group, would like to thank ESI Group and in particular Dr Vincent Chaillou, COO, for giving him free access to ESI Group's powerful IT tools and resources.

References

[1] "APPENDIX 1.12A-2 - DEBRIS EXAMINATION, ITEM 1 – FLAPERON", *Safety Investigation Report MH370 (9M-MRO)*, Direction Générale De L'Armement (DGA), Ministère de La Défense, Sept. 2015

[2] Kamoulakos, A., "Aspects of analysis and simulation of a flaperon ditching scenario", *AIAA AVIATION 2020 FORUM*, June 15-19, 2020, VIRTUAL EVENT

[3] Kamoulakos, A., Marchand, J-L., Gasser, P., Delarche, M., and Garot, J-M., "La Fin du Vol MH370 : Un Amerrissage Forcé, Étude du Flaperon Heurtant la Surface de la Mer", *LETTRE 3AF Numéro 41*, Association Aéronautique et Astronautique de France (3AF), Jan - Feb 2020. (English version available at the CAPTIO website http://mh370-captio.net/)

[4] Von Karman, T., "The Impact of Seaplane Floats During Landing", *NACA TN 321*, Oct 1929.

[5] Wagner, H., "Landing of Seaplanes", *NACA TM 622*, Jan 1931

[6] Mayo, W., L., "Analysis and Modification of Theory for Impact of Seaplanes on Water", *NACA Report No. 810*, NASA Langley Laboratory, Aug 1945

[7] Smiley, R., F., "A Semiempirical Procedure for Computing the Water Pressure Distribution on Flat and V-Bottom Prismatic Surfaces During Impact or Planing" *NACA TN 2583*, NASA Langley Laboratory, Dec 1951

[8] Szebehely, V., G., "Hydrodynamics of Slamming Ships", *Report 823*, Navy Department, July 1952

[9] Payne, P., R., "The Vertical Impact of a Wedge on a Fluid", *Ocean Engineering*, Vol 8, No. 4, pp. 421-436, Pergamon Press, 1981

[10] VPS (PAMCRASH) User's Manual, ESI Group

[11] Smiley, R., F., "An Experimental Study of Water-Pressure Distributions During Landings and Planning of a Heavily Loaded Rectangular Flat-Plate Model" *NACA TN 2453*, NASA Langley Laboratory, Sep 1951

[12] Smiley, R., F., "Water-Pressure Distributions During Landings of a Prismatic Model Having an Angle of Dead Rise of 22.5 degrees and Beam-Loading Coefficients of 0.48 and 0.97" *NACA TN 2816*, NASA Langley Laboratory, Nov 1952

[13] Smiley, R., F., "A Study of Water Pressure Distributions During Landings with Special Reference to a Prismatic Model Having a Heavy Beam Loading and a 30 degrees angle of Dead Rise" *NACA TN 2111*, NASA Langley Laboratory, Jul 1950

[14] Kamoulakos, A., "Stability Analysis of Flexible Wind Turbine Blades Using the Finite Element Method" *NASA CR-168107*, NASA Lewis Research Center, August 1982